molecules

MDPI

Article

The Dichotomy of Mn–H Bond Cleavage and Kinetic Hydricity of Tricarbonyl Manganese Hydride Complexes

Elena S. Osipova [1], Sergey A. Kovalenko [1], Ekaterina S. Gulyaeva [1,2], Nikolay V. Kireev [1], Alexander A. Pavlov [1,3], Oleg A. Filippov [1], Anastasia A. Danshina [1,4], Dmitry A. Valyaev [2,*], Yves Canac [2], Elena S. Shubina [1] and Natalia V. Belkova [1,*]

[1] A.N. Nesmeyanov Institute of Organoelement Compounds, Russian Academy of Sciences (INEOS RAS), 28, Vavilova Str., 119334 Moscow, Russia; aosipova92@gmail.com (E.S.O.); kovalenko2000as@gmail.com (S.A.K.); elenor.kagami@gmail.com (E.S.G.); shu@ineos.ac.ru (E.S.S.)
[2] LCC-CNRS, Université de Toulouse, CNRS, 205 Route de Narbonne, CEDEX 4, 31077 Toulouse, France
[3] Center of National Technological Initiative, Bauman Moscow State Technical University, 2nd Baumanskaya Str., 5, 105005 Moscow, Russia
[4] Moscow Institute of Physics and Technology, Institutskiy per., 9, 141700 Dolgoprudny, Russia
* Correspondence: dmitry.valyaev@lcc-toulouse.fr (D.A.V.); nataliabelk@ineos.ac.ru (N.V.B.)

Abstract: Acid-base characteristics (acidity, p*K*a, and hydricity, ΔG°_{H-} or k_{H-}) of metal hydride complexes could be a helpful value for forecasting their activity in various catalytic reactions. Polarity of the M–H bond may change radically at the stage of formation of a non-covalent adduct with an acidic/basic partner. This stage is responsible for subsequent hydrogen ion (hydride or proton) transfer. Here, the reaction of tricarbonyl manganese hydrides *mer*,*trans*–[$L_2Mn(CO)_3H$] (**1**; L = $P(OPh)_3$, **2**; L = PPh_3) and *fac*–[(L–L′)$Mn(CO)_3H$] (**3**, L–L′ = $Ph_2PCH_2PPh_2$ (dppm); **4**, L–L′ = Ph_2PCH_2–NHC) with organic bases and Lewis acid ($B(C_6F_5)_3$) was explored by spectroscopic (IR, NMR) methods to find the conditions for the Mn–H bond repolarization. Complex **1**, bearing phosphite ligands, features acidic properties (p*K*a 21.3) but can serve also as a hydride donor ($\Delta G^{\neq}_{298K}$ = 19.8 kcal/mol). Complex **3** with pronounced hydride character can be deprotonated with KHMDS at the CH_2–bridge position in THF and at the Mn–H position in MeCN. The kinetic hydricity of manganese complexes **1**–**4** increases in the order *mer*,*trans*–[$(P(OPh)_3)_2Mn(CO)_3H$] (**1**) < *mer*,*trans*–[$(PPh_3)_2Mn(CO)_3H$] (**2**) ≈ *fac*–[(dppm)$Mn(CO)_3H$] (**3**) < *fac*–[$(Ph_2PCH_2NHC)Mn(CO)_3H$] (**4**), corresponding to the gain of the phosphorus ligand electron-donor properties.

Keywords: manganese hydrides; hydrogen bond; non-covalent interactions; proton transfer; hydride transfer; hydricity

Citation: Osipova, E.S.; Kovalenko, S.A.; Gulyaeva, E.S.; Kireev, N.V.; Pavlov, A.A.; Filippov, O.A.; Danshina, A.A.; Valyaev, D.A.; Canac, Y.; Shubina, E.S.; et al. The Dichotomy of Mn–H Bond Cleavage and Kinetic Hydricity of Tricarbonyl Manganese Hydride Complexes. *Molecules* **2023**, *28*, 3368. https://doi.org/10.3390/molecules28083368

Academic Editor: Zi-Jian Yao

Received: 16 March 2023
Revised: 4 April 2023
Accepted: 8 April 2023
Published: 11 April 2023

1. Introduction

A search for inexpensive and efficient catalysts that give more sustainable alternatives to platinum group metals recently led to remarkable progress in the development of catalytic systems based on organometallic manganese complexes [1,2]. While pincer-type Mn(I) derivatives still dominate in the field of catalytic (de)hydrogenation, it was demonstrated that less elaborated bidentate systems *fac*–[(L–L′)$Mn(CO)_3Br$] may also be highly efficient [3]. Generally, the formation of catalytically relevant transition metal hydrides from the corresponding bromide precursors proceeds in situ in the presence of various basic additives. This activation step can be nicely illustrated for Mn(I) complexes *fac*–[(P–NHC)$Mn(CO)_3Br$] (P–NHC = κ^2P,C–Ph_2PCH_2–NHC) [4] and *fac*–[$(dppm^R)Mn(CO)_3Br$] (dppm = κ^2P,P–$Ph_2PCH(R)PPh_2$, R = H, Me, Ph) [5] in the presence of KHMDS leading to the formation of cyclometalated species capable of activating dihydrogen via unconventional metal-ligand cooperation. The resulting hydride products *fac*–[(L–L′)$Mn(CO)_3H$] interact with organic substrates to form non-covalent adducts and typically the formation

of such intermediates directly precedes hydride/proton transfer steps providing *in fine* the hydrogenation of polar C=X bonds.

It is generally accepted that transition metal hydrides can be proton, hydride or hydrogen atom donors [6–8]. However, the vast majority of hydride complexes exhibit only one reactivity mode being determined by the nature of auxiliary ligands and relative charge on the core metal atom [9]. Nevertheless, there are a few families of hydrides in which the same hydride complex possesses distinct reactivity. *Dual* reactivity is well documented, for example, for groups 6–8 metal complexes [$CpM(CO)_3H$] (M = Mo, W), [$(CO)_5MH$] (M = Mn, Re) and [$CpM(CO)_2H$] (M = Fe, Ru, Os) [8,10–12]. Whether the M–H bond releases a proton or hydride, obviously, depends on the partner reagent. We have shown for the first time that the M–H bond polarity gets adjusted at the stage of a non-covalent complex formation preceding the M–H bond dissociation [13] (Scheme 1).

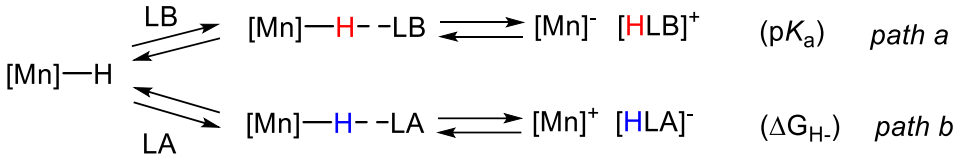

Scheme 1. LB = Lewis base, LA = Lewis acid.

The acidity and hydricity of the M–H bond can be quantified in terms of pK_a and ΔG°_{H-}, respectively [14–16]. The quantitative scale of kinetic hydricity (k_{H-}) has been developed for group 6–7 metal hydrides in the pioneering work of Bullock [11]. However, the data for manganese complexes are still scarce despite their utility as potential catalysts. Experimental values of acidity and hydricity are known only for [$(CO)_5MnH$] (pK_a = 14.2 in MeCN [8], ΔG°_{H-} = 59.61 kcal/mol [17], k_{H-} = 50 $M^{-1}s^{-1}$ [11]), [$(CO)_4(C_6H_6)MnH$] (pK_a = 26.8 in MeCN [8]) and *cis*–[$(CO)_4(PPh_3)MnH$] (pK_a = 20.4 in MeCN [8], k_{H-} = 230 $M^{-1}s^{-1}$ [11]). There is a sole theoretical work devoted to a systematic study of $(CO)_5MnH$ and $(CO)_{5-n}(PH_3)_nMnH$ complexes [17] demonstrating that the hydricity of the metal hydride bond is greatly amplified when the CO ligand is replaced by a phosphine donor [17].

The research presented herein explores the dichotomy of Mn–H bond cleavage and the potential of its repolarization entailed by intermolecular interactions with Lewis acids and bases. By gaining an understanding of the acid-base characteristics of different manganese hydrides, it should be possible to forecast their catalytic performance and drive the catalyst design.

In this context, we chose two types of octahedral Mn(I) hydride complexes (Scheme 2) in which the Mn–H bond is expected to have different polarity. Electron-deficient phosphite ligands in complex *mer*,*trans*–[$(P(OPh)_3)_2Mn(CO)_3H$] (**1**) and more donating triarylphosphines in complex *mer*,*trans*–[$(PPh_3)_2Mn(CO)_3H$] (**2**) should provide them an acidic and basic character, respectively. In agreement with our expectations, complex **1** can be deprotonated by *t*BuOK [18], and complex **2** exhibits typical reactivity of "hydridic" hydride releasing H_2 [19,20] upon protonation by $HBF_4{\cdot}Et_2O$ [21]. The incorporation of chelating and more electron-rich ligands such as bidentate phosphine in *fac*–[(dppm)$Mn(CO)_3H$] (**3**) or phosphine–N–Heterocyclic carbene in *fac*–[(P–NHC)$Mn(CO)_3H$] (**4**) ought to increase the Mn–H basicity and hydride donating ability (Scheme 2). The acidity and hydricity of **1**–**4** have not been evaluated before this work; therefore, the entire set of these complexes could be used to create the scale of their thermodynamic/kinetic hydricity by evaluating the impact of the ligand.

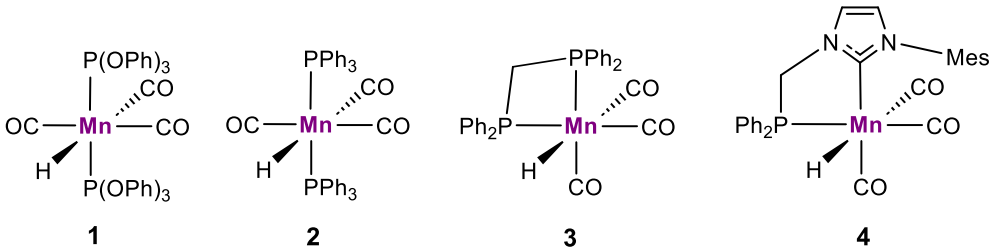

Scheme 2. Representation of the Mn–H complexes **1**–**4** which are the subject of this study.

2. Results and Discussion

2.1. Interaction of Tricarbonyl Manganese Hydrides **1**–**4** *with Bases*

Hydrogen bonding. Addition of Lewis bases (LB) such as pyridine and hexamethylphosphoramide (HMPA) to complex *mer*,*trans*–[$(P(OPh)_3)_2Mn(CO)_3H$] (**1**) in methylcyclohexane (MCH) at 190 K leads to weak hydrogen bond formation where Mn–H serves as a proton donor [22–25]. Hydrogen bonding was evidenced by the appearance of a low-frequency shoulder at the initial ν_{CO} 1958 cm^{-1} band ($\Delta\nu$ 5–20 cm^{-1}) (Figure S1). Since hydrogen bonding is a reversible process, a temperature increase up to 290 K shifts the equilibrium (Scheme 1, path a) towards free manganese hydride. Complex *fac*–[(dppm)$Mn(CO)_3H$] (**3**) also forms a hydrogen bond with these bases; its three ν_{CO} bands (1996, 1916, 1909 cm^{-1}) shift to lower frequencies by 3–7 cm^{-1} in the presence of 70 equiv. HMPA (Figure S2). However, the strength of these bases is insufficient for proton transfer to occur. The change of the nonpolar MCH to polar acetonitrile also does not promote the proton transfer from **3** to pyridine (pK_a = 12.53 in MeCN) or HMPA (pK_a = 6.1 in CH_3NO_2).

Proton transfer. Quantitative deprotonation of **1** was observed in acetonitrile when a stronger base—1,8–diazabicyclo[5.4.0]undec–7–ene (DBU; pK_a = 24.31 in MeCN)—was used. Full conversion of **1** to anionic complex $[(P(OPh)_3)_2Mn(CO)_3]^-[HDBU]^+$ ($\mathbf{1}^-$) was confirmed by ^{31}P NMR in CD_3CN, since the initial signal at δ_P 183.3 ppm converts into downfield resonance δ_P 206.5 ppm after DBU addition (the key spectral parameters for this and all other complexes studied are summarized in Table 1). To explore the features of proton transfer equilibrium (Scheme 1, path a), we decided to return into a non-polar solvent that should impede proton transfer process. Indeed, in methylcyclohexane the proton transfer is temperature dependent and starts when the reaction mixture is cooled below 260 K. According to IR spectra, the addition of 1.1 equiv. DBU to a solution of **1** in MCH at low temperatures (190–260 K) leads to the appearance of anionic manganese species $[(P(OPh)_3)_2Mn(CO)_3]^-$ ($\mathbf{1}^-$, ν_{CO} 1815 cm^{-1}) at the expense of the initial complex (ν_{CO} 1958 cm^{-1}). Unexpectedly, proton transfer is slow at these temperatures, taking 1.2 h at 230 K to reach the equilibrium (Figure S3). The rate constants analysis gave the activation energies (See Supplementary Materials for more details) for the proton transfer step: $\Delta H^{\neq}$ = 7.5 kcal/mol, $\Delta S^{\neq}$ = −26 cal/(mol·K), $\Delta G^{\neq}_{298K}$ = 15.3 kcal/mol. Since the system does come to equilibrium, the experimental equilibrium constants with thermodynamic parameters of proton transfer in MCH were obtained: ΔH° = −13.1 kcal/mol, ΔS° = −50 cal/(mol·K), ΔG°_{298K} = 1.9 kcal/mol (See Supplementary Materials for more details). The reaction of **1** with a slightly weaker base $[Bu_4N]^+[4–NO_2C_6H_4O]^-$ (pK_a = 20.7 in MeCN [26]) immediately reaches equilibrium in MeCN with the formation of only ~30% proton transfer product (Figure S4). The known acidity constant of $4–NO_2C_6H_4OH$ allows an estimation of complex **1** acidity pK_a(**1**) = 21.3.

Table 1. IR and $^{31}P\{^{1}H\}$ NMR data for neutral, cationic and anionic manganese species **1**–**4** in different solvents.

Complex	ν_{CO} (cm^{-1})	δ_P (ppm)
1, $[(P(OPh)_3)_2Mn(CO)_3H]$	2040 w, 2028 w, 1956 s [a] 2041 w, 2028 w, 1955 s [b] 2043 w, 2031 w, 1958 s [c]	183.3
$\mathbf{1^+}$, $[(P(OPh)_3)_2Mn(CO)_3][HB(C_6F_5)_3]$	2011 s, 1969 s [a]	153.5
$\mathbf{1^-}$, $[(P(OPh)_3)_2Mn(CO)_3][HDBU]$	1815 s [c]	206.5
2, $[(PPh_3)_2Mn(CO)_3H]$	1908 s, 1900 s [f]	80.5
$\mathbf{2^+}$, $[(PPh_3)_2Mn(CO)_3]^+[HB(C_6F_5)_3]^-$	1980 s, 1930 s [f]	61.8
$\mathbf{2^-}$, $[(PPh_3)_2Mn(CO)_3]^-[K^+]$	1770 s, 1741 s [e]	-
3, $[(dppm)Mn(CO)_3H]$	1996 s, 1916 s, 1909 s [a] 1993 s, 1914 s, 1903 s [b]	30.1 [a] 31.8 [b]
fac-$\mathbf{3^+}$, $[(dppm)Mn(CO)_3)][HB(C_6F_5)_3]$ [27]	2040 s, 1973 s, 1935 s [d]	10.1
mer-$\mathbf{3^+}$, $[(dppm)Mn(CO)_3)][HB(C_6F_5)_3]$ [27]	2060 s, 2003 s [d]	10.6, 7.1
$\mathbf{3^{CH-}}$, *fac*–$[(CH^-$-dppm$)Mn(CO)_3H][K^+]$	1957 s, 1871 s, 1876 s [e] 1956 s, 1870 s [b]	10.9 [a]
$\mathbf{3^{Mn-}}$, $[(dppm)Mn^-(CO)_3][K^+]$	1867 s, 1779 s [b]	29.9 [b]
4, *fac*–[(P–NHC)$Mn(CO)_3H$]	1989 s, 1909 s, 1889 s [a] 1988 s, 1907 s,1888 s [d]	95.8
fac-$\mathbf{4^+}$, $[(P–NHC)Mn(CO)_3][HB(C_6F_5)_3]$	2032 s, 1949 s, 1921 s [d]	78.1, 71.1 [f]
mer-$\mathbf{4^+}$, $[(P–NHC)Mn(CO)_3][HB(C_6F_5)_3]$	2038 s, 1968 s, 1942 s [d]	-

[a] toluene, [b] MeCN, [c] MCH, [d] *n*BuCl, [e] THF, [f] CH_2Cl_2.

Manganese catalyzed transfer hydrogenation reactions are usually carried out in the presence of strong bases such as potassium *tert*-butylate or KHMDS [1,3,4]. A possible reaction mechanism includes Mn–H bond deprotonation with formation of anionic complex, which participates in further catalytic transformations [3]. We have tried multiple times to identify the conditions for proton abstraction from *mer*,*trans*–$[(PPh_3)_2Mn(CO)_3H]$ (**2**) and *fac*–$[(dppm)Mn(CO)_3H]$ (**3**), where the Mn–H bond is expected to be rather electron-rich due to the presence of phosphine ligands. However, no repolarization of the Mn–H bond and proton transfer was observed for hydride complexes **2** and **3** with various bases (pyridine, HMPA, DBU, TBD (1,5,7–triazabicyclo[4.4.0]dec–5–ene, pK_a = 26.03 in MeCN [28])) even in polar solvents (MeCN, THF). Fortunately, treatment of complex **2** at ambient temperature in THF with KHMDS excess (2 equiv., pK_a = 26 in THF [29]) led to partial proton transfer indicated by the appearance of two new low-frequency ν_{CO} bands at 1770 and 1741 cm^{-1} in IR spectrum that correspond to anionic complex $\mathbf{2^-}$ (Figure S5) [30]. From these spectral data the pK_a value 27.3 for manganese hydride **2** in THF was estimated.

The reaction of hydride complex **3** with KHMDS (5 equiv.) in THF leads to full proton transfer and the appearance of three new low-frequency-shifted CO bands (1957, 1871, 1876 cm^{-1}) in the IR spectra (Figure 1). The shift of ν_{CO} bands by ca. 40 cm^{-1} in the IR spectra is not consistent with the presence of the negative charge at the metal atom in the case of Mn–H bond deprotonation. Moreover, ^1H NMR spectrum shows the presence of a triplet signal at δ_H −5.54 ppm in the hydride region, while for the initial complex **3** the hydride signal (δ_H −5.53 ppm) is a triplet of doublets due to the $^2J_{PH}$ and an additional $^4J_{HH}$ spin-spin interaction with one of the CH_2 bridge H-atoms. The phosphorus resonance observed in this **3**/KHMDS mixture by $^{31}P\{^1H\}$ NMR spectroscopy is shifted to stronger field (δ_P 10.9) relative to that (δ_P 30.1) of the initial manganese hydride **3** (Figure S6). These spectral data allow the proposal that deprotonation occurs at the bridging CH_2 group of dppm ligand with the formation of $[\mathbf{3^{CH-}}][K^+]$. In the ^{13}C spectrum, the triplet

(δ_C 20.8, t, $^1J_{CP}$ = 51.4 Hz, PC*H*P) of corresponding anionic carbon CH^- is also shifted to stronger field compared to the CH_2 signal of **3** (δ_C 48.0, t, $^1J_{CP}$ = 22.4 Hz, PCH_2P). The estimated pK_a value of methylene CH-proton in complex **3** equals 26 in THF. A more polar acetonitrile deprotonation of **3** by the same amount of KHMDS goes through [$\mathbf{3}^{CH-}$][K^+] formation yielding ultimately the anionic manganese complex [$\mathbf{3}^{Mn-}$][K^+] (Scheme 3). In the IR and NMR spectra, measured immediately after mixing, three manganese species could be observed; however, in 15 min, the intermediate [$\mathbf{3}^{CH-}$][K^+] (ν_{CO} 1956, 1870 cm^{-1}; δ_P 10.4 ppm) completely transforms into the final species [$\mathbf{3}^{Mn-}$][K^+] ((ν_{CO} 1867, 1779 cm^{-1}; δ_P 29.9 ppm) (Figure 1 and Figure S6) that has no hydride signal in the ^1H NMR spectrum. According to our DFT calculations, the intramolecular proton transfer from manganese to the anionic bridge CH^- is explained by thermodynamic preference of the metal deprotonated form (ΔG_{298K} = −0.2 kcal/mol) in acetonitrile compared with THF (Table 2). That implies that even manganese complexes with pronounced hydride character [11,17] can be deprotonated by KHMDS, thus allowing the corresponding anionic intermediates to participate in hydrogenation reactions.

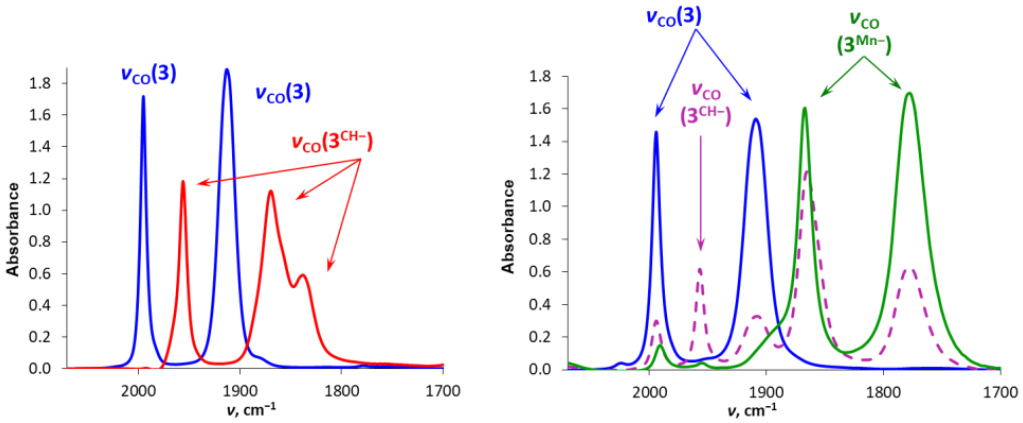

Figure 1. IR spectra of *fac*–[(dppm)Mn(CO)$_3$H] (**3**) (c = 0.01 M) alone (blue) and after KHMDS addition (5 equiv.; red/green). (**Left**)—THF, (**right**)—MeCN (l = 0.01 cm, 295 K).

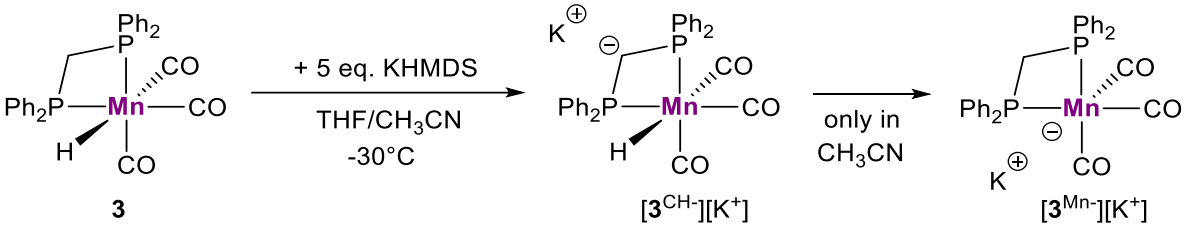

Scheme 3. Formation of [$\mathbf{3}^{Mn-}$][K^+] from **3** by addition of KHMDS.

Table 2. Relative energies (in kcal/mol) of the complex [$\mathbf{3}^{Mn-}$][K^+] formation computed at DFT/ωB97XD/def2-TZVP level. Complex [$\mathbf{3}^{Mn-}$][K^+] is taken as a zero.

	Toluene	THF	MeCN
E_{el}	+2.8	−0.7	−3.1
ΔH	+5.7	+2.0	−0.2
ΔG	+7.6	+2.5	−0.2

2.2. Interaction of Tricarbonyl Manganese Hydrides with Lewis Acids

Non-covalent adducts. Interaction of manganese hydride complexes (**1**–**4**) with Lewis acids (**LA**) leads to Mn–H bond polarization, making the hydride atom more negatively charged. Recently, we have proven that the formation of non-covalent adducts between Lewis acid and hydride complex *fac*–[(dppm)Mn(CO)$_3$H] (**3**) at 180 K precedes the hydride

ion abstraction [27] (Scheme 4). Noteworthy, while the initial hydride **3** has *facial* geometry, the most stable form of the non-covalent adduct is the isomer with the *meridional* geometry. The latter then undergoes additional transformations, including intramolecular hydride transfer with the formation of *meridional* cation stabilized by the solvent molecule *mer*–[(dppm)Mn(CO)$_3$(κ^1*Cl*–CH$_2$Cl$_2$)](HBAr$_3$) and its isomerization to a more stable *facial* isomer *fac*–[(dppm)Mn(CO)$_3$(κ^1*Cl*–CH$_2$Cl$_2$)](HBAr$_3$).

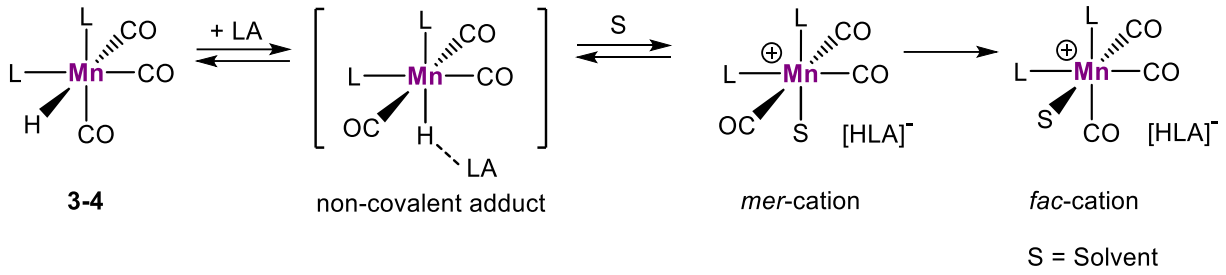

Scheme 4. Isomerization process of complexes **3**–**4** into more stable *facial* isomers.

The analogous chemical behavior was observed upon addition of B(C$_6$F$_5$)$_3$ to complex *fac*–[(P–NHC)Mn(CO)$_3$H] (**4**) at 180 K in methylene chloride. The Lewis acid coordination to the hydride ligand and formation of the non-covalent adduct **4**···LA gives in ^{1}H NMR spectrum a broadened resonance at δ_H −7.98 ppm shifted high-field relative to the initial signal of **4** (δ_H −7.42) (Figure 2). A weak BrØnsted acid *mer*,*trans*–[(P(OPh)$_3$)$_2$Mn(CO)$_3$H] (**1**) also interacts with Lewis acids as a hydride-ion donor. Addition of B(C$_6$F$_5$)$_3$ (10 equiv.) to the toluene solution of **1** (ν_{CO} 2040 w, 2028 w, 1956 s cm^{-1}) at 190 K leads to the formation of a non-covalent complex **1**···B(C$_6$F$_5$)$_3$ (ν_{CO} 2035 s, 1973 s cm^{-1}). We assume that this adduct has a *facial* configuration, since its ν_{CO} bands are strongly shifted to high frequencies (*cf*. 2046 s, 1980 s cm^{-1} for *fac*-**1** and 2026 w, 1942 s cm^{-1} for *mer*,*trans*-**1** in nujol) [31]. Formation of non-covalent adduct with B(C$_6$F$_5$)$_3$ stabilizes *fac*-**1** and in the 190–220 K temperature range the equilibrium between two species, *mer*,*trans*-**1** and *fac*-**1**···B(C$_6$F$_5$)$_3$, is observed in the IR spectra (Figure S7). In ^{1}H NMR spectra of the **1** + B(C$_6$F$_5$)$_3$ mixture, measured under the same conditions, the formation of the intermediate complex *fac*-**1**···B(C$_6$F$_5$)$_3$ is evidenced by new broad hydride resonance shifted to the higher field (δ_H −9.36 ppm) (Figure S8, left). In ^{31}P{^{1}H} NMR spectra (Figure S8, right), the resonance at δ_P 163 ppm exhibits the same temperature behavior and can be attributed to *fac*-**1**···B(C$_6$F$_5$)$_3$. Thus, complex **1** is the least reactive toward hydride transfer (see below) and its non-covalent adduct with Lewis acid exists in a wider temperature range.

Hydride transfer. The non-covalent adducts **1**···LA–**4**···LA precede the intramolecular hydride transfer that yields the cationic complexes with different geometries, which are stabilized by coordination of solvent molecule or [H-LA]$^-$ anion. Thus, for *fac*–[(P–NHC)Mn(CO)$_3$H] (**4**) interacting with B(C$_6$F$_5$)$_3$ at 180 K, new high-frequency ν_{CO} bands at 2038, 1968 and 1942 cm^{-1} appear in the IR spectrum assigned to the cationic *mer*-intermediate; at 190 K they already transform into *fac*-product with ν_{CO} bands at 2032, 1949 and 1921 cm^{-1} (Figure S9). In contrast to isostructural *fac*–[(dppm)Mn(CO)$_3$H] (**3**), in the case of complex **4** two configurations are possible when Mn(CO)$_3$ moiety is in meridional arrangement: hydride ligand being *trans* to the phosphorus atom (*mer*-P-**4**) or *trans* to the NHC carbon atom (*mer*-C-**4**) (Figure S8). Since complex *mer*-P-**4** should feature more hydridic H-atom than *mer*-C-**4** due to the higher *trans*-effect of phosphorus [32], we assumed that the hydride transfer occurs through the formation of the meridional *trans*-to-P form (*mer*-P-**4**···B(C$_6$F$_5$)$_3$).

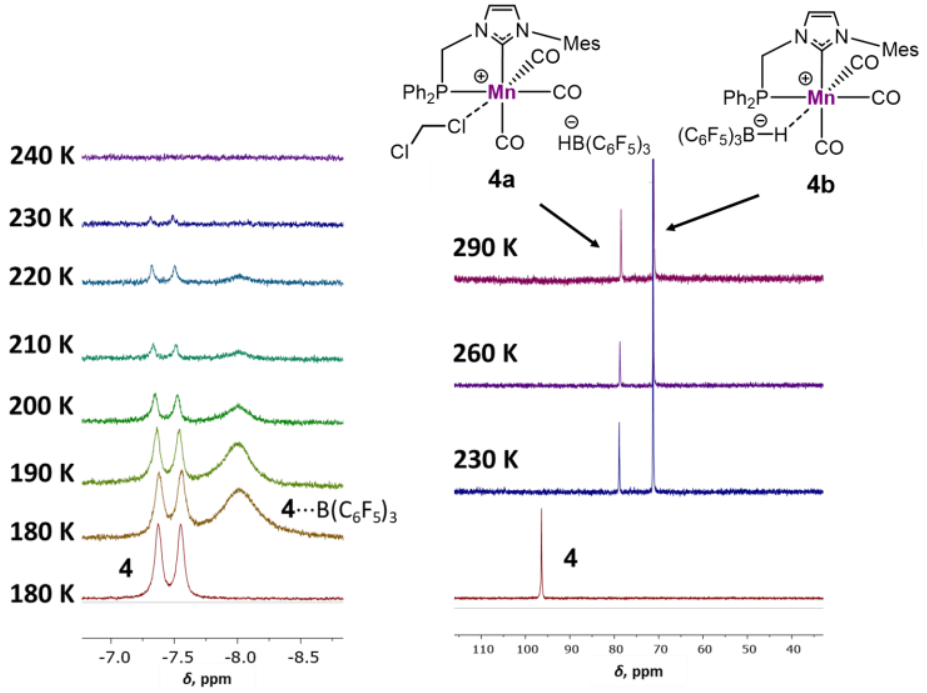

Figure 2. Variable temperature ^{1}H (300 MHz) and ^{31}P{^{1}H} (162.0 MHz) NMR spectra of complex **4** in CD_2Cl_2 solution (bottom lines) and its mixture with $B(C_6F_5)_3$.

Above 230 K, the equilibrium is completely shifted to cationic products, the ^{31}P{^{1}H} spectrum contains only two resonances δ_P 78.0 and 71.0 ppm in 1:4 ratio (Figure 2). After 4 days at room temperature, this ratio inverts and becomes 2:1. By selectively decoupling ^{31}P, the CH_2-bridge H-atoms δ_H 5.07 (dd, $^{2}J_{HH}$ = 14.0, $^{2}J_{PH}$ = 5.1 Hz) and 4.94 (dd, $^{2}J_{HH}$ = 14.1, $^{2}J_{PH}$ = 6.6 Hz) can be attributed to complex **4a** with δ_P 78.1 ppm and δ_H 5.48 (vt, $^{2}J_{HH}$ = 14.4 Hz, $^{2}J_{PH}$ = 13.7 Hz) and 4.99 (d, $^{2}J_{HH}$ = 14.4 Hz) to complex **4b** δ_P 71.1. While the ^{31}P{^{1}H} resonance of **4a** shifts (between 74.1 and 78.1 ppm) in response to changing the solvent (toluene, *n*BuCl, C_6H_5Cl, CD_2Cl_2), the chemical shift of **4b** keeps its position (Table S1). Thus, we suggest that the two cationic products are [(P–NHC)Mn(CO)$_3$(Solvent)][HB(C_6F_5)$_3$)] (**4a**), which has a coordinated solvent molecule, and [(P–NHC)Mn(CO)$_3$][HB(C_6F_5)$_3$)] (**4b**), which is a contact ionic pair stabilized by B–H bond interaction with the cationic metal center (**4b**) remains in tranquility. The sensitivity of the ^{31}P{^{1}H} resonance of **4a** to the media is indicative of the solvent's influence on its structure. To obtain an independent proof of its structure, we reacted the manganese bromide *fac*–[(P–NHC)Mn(CO)$_3$Br] with $AgBF_4$ in MeCN as a solvent. The cationic complex $\mathbf{4^{MeCN}}$ obtained features acetonitrile molecule coordinated to the metal center as it was confirmed by X-ray diffraction (Figure 3), and its ^{31}P{^{1}H} resonance (77.5 ppm in CD_2Cl_2) is in the range of **4a**-type complexes.

For the non-covalent complex *fac*-**1**$\cdots$B(C_6F_5)$_3$ the hydride transfer occurs above 230 K (Scheme 5). The single product of the hydride transfer is a cationic manganese complex *mer*,*trans*–[1]$^+$[HB(C_6F_5)$_3$]. The signal of the cationic product [1]$^+$[HB(C_6F_5)$_3$]$^-$ becomes clearly seen in ^{31}P spectra at 250 K (δ_P 153.0 ppm).

Structurally similar complex *mer*,*trans*–[(PPh_3)$_2$Mn(CO)$_3$H] (**2**) bearing more donating phosphine ligands was found to be more reactive. Indeed, it transforms into *mer*,*trans*–[(PPh_3)$_2$Mn(CO)$_3$(solv)][HB(C_6F_5)$_3$] (**2**$^+$) already at 180 K (Figure S11). IR spectra in the 180–250 K range show the transformation of hydride **2** directly into cationic complex [**2**$^+$][HB(C_6F_5)$_3$] (ν_{CO} 1980, 1930 cm^{-1}) without detectable non-covalent adduct formation and *mer*-to-*fac* isomerization. At temperatures higher than 250 K, partial decomposition of this cationic species was observed, resulting in the formation of known tetracarbonyl complex *trans*–[(PPh_3)$_2$Mn(CO)$_4$]$^+$ exhibiting a ν_{CO} band at 2002 cm^{-1} [33]. ^{31}P{^{1}H} NMR spectra confirm the formation of sole cationic product (δ_P 61.8 ppm) and its further decomposition. Direct synthesis of *mer*,*trans*–[(PPh_3)$_2$Mn(CO)$_3$(CH_3CN)]$^+$[BF_4]$^-$ $\mathbf{2^{MeCN}}$ allows

the formation of a stable cationic product with ν_{CO} at 2055 w, 1977 s, 1946 s cm^{-1} characterized by X-ray diffraction (Figure 4).

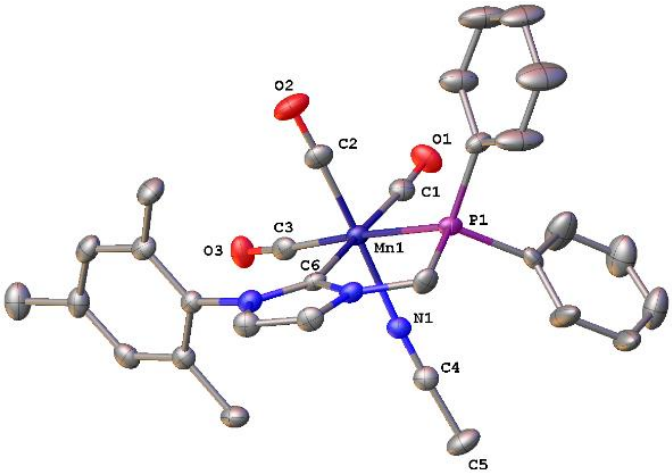

Figure 3. Molecular structure of the cationic complex *fac*–[(P–NHC)Mn(CO)$_3$(MeCN)]$^+$[BF$_4$]$^-$ (**4**^{MeCN}) (40% probability ellipsoids, only one crystallographically independent molecule in the cell is shown). Counter-anions and hydrogen atoms are omitted for clarity. Selected bond lengths (Å): Mn1-N1 2.011(4), Mn1-P1 2.317(1), Mn1-C6 2.048(5), C1-O1 1.146(7), C2-O2 1.156(6), C3-O3 1.146(5), Mn1-C1 1.817(6), Mn1-C2 1.786(5), Mn1-C3 1.835(4), N1-C4 1.130(6).

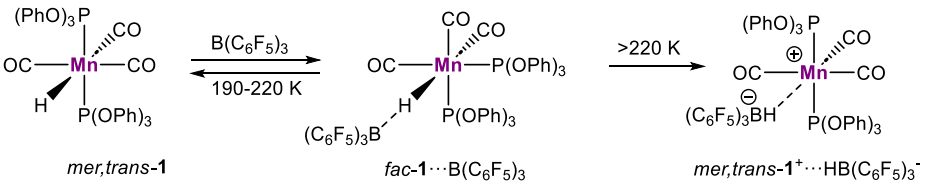

Scheme 5. Formation of complex *mer*,*trans*–[1]$^+$[HB(C$_6$F$_5$)$_3$] from **1** in the presence of B(C$_6$F$_5$)$_3$.

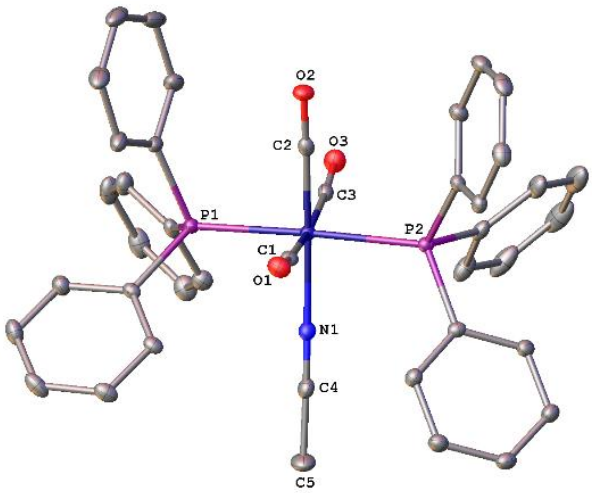

Figure 4. Molecular structure of the cationic complex *mer*,*trans*–[(PPh$_3$)$_2$Mn(CO)$_3$(CH$_3$CN)]$^+$ **2**^{MeCN} (40% probability ellipsoids, tetrafluoroborate anion, solvate molecule of dichloromethane and hydrogen atoms are omitted for clarity). Selected bond lengths (Å): Mn1-N1 1.999(3), Mn1-P1 2.3337(8), Mn1-P2 2.3329(8), C1-O1 1.140(3), C2-O2 1.149(4), C3-O3 1.137(3), Mn1-C1 1.857(3), Mn1-C2 1.794(3), Mn1-C3 1.860(4), N1-C4 1.134(4).

2.3. Kinetic Hydricity of Manganese Tricarbonyl Complexes

The hydride transfer from complexes **1**–**4** to $B(C_6F_5)_3$ is relatively slow at low temperatures that allow the estimation of their kinetic hydricities (See Supplementary Materials for more details; Figures S12 and S13). The low-temperature IR monitoring of hydride transfer kinetics in the presence of 1.1 equiv. $B(C_6F_5)_3$ in *n*BuCl gave effective rate constants (k_{eff}). The value of free energy $\Delta G^{\neq}_{298K}$ characterizes the kinetic hydricity of manganese complexes but depends on the Lewis acidity of the given hydride abstractor. As expected, the hydride complex **1**, which is a weak acid due to electron-withdrawing phosphite ligands, has the lowest hydricity ($\Delta G^{\neq}_{298K}$ = 19.8 kcal/mol), while complex **4** bearing phosphine-carbene ligand, the most electron-rich in this series, possesses the highest hydricity ($\Delta G^{\neq}_{298K}$ = 16.5 kcal/mol) among the complexes studied (Table 3). The kinetic hydricity of the manganese complexes of interest increases in the order *mer*,*trans*–$[(P(OPh)_3)_2Mn(CO)_3H]$ (**1**) < *mer*,*trans*–$[(PPh_3)_2Mn(CO)_3H]$ (**2**) ≈ *fac*–$[(dppm)Mn(CO)_3H]$ (**3**) < *fac*–$[(P\text{-}NHC)Mn(CO)_3H]$ (**4**), reflecting the gain of the phosphorus ligand electron donor properties (basicity). On the activation free energy scale ($\Delta G^{\neq}_{298K}$) there is only small by 0.5 kcal/mol difference between complexes **2**–**4** bearing electron-donating ligands. However, the distinction between their properties becomes more pronounced at lower temperatures due to the impact of highly negative activation entropy $\Delta S^{\neq}$ (cf. $k_{eff\ 220K}$, Table 3).

Table 3. Effective rate constants for the interaction between **1**–**4** and $B(C_6F_5)_3$ in *n*BuCl at 220 K and activation parameters of hydride transfer.

MnH	k_{eff} 220K, $M^{-1}\cdot s^{-1}$	$\Delta H^{\neq}$, kcal/mol	$\Delta S^{\neq}$, cal/(mol·K)	$\Delta G^{\neq}_{220K}$, kcal/mol	$\Delta G^{\neq}_{298K}$, kcal/mol
1	0.00008	8.6 ± 0.2	−37 ± 1	16.9 ± 0.1	19.8 ± 0.1
2	0.147	4.1 ± 0.5	−43 ± 3	13.6 ± 0.3	17.0 ± 0.3
3	0.006	9.4 ± 0.6	−26 ± 3	15.0 ± 0.2	17.0 ± 0.2
4	0.706	3.8 ± 0.2	−43 ± 1	13.2 ± 0.1	16.5 ± 0.1

3. Materials and Methods

All reactions were performed using standard Schlenk procedures under a dry argon atmosphere. Dry and oxygen-free organic solvents (toluene, THF) were obtained using a solvent purification system from M. Braun (Garching, Germany). Methylcyclohexane was dried over Na and distilled under an argon atmosphere. *n*BuCl, CH_2Cl_2 and acetonitrile were stored over CaH_2 and distilled under an argon atmosphere before use. Deuterated solvents for NMR were degassed before use by three freeze–pump–thaw cycles and kept over 3Å molecular sieves. A liquid nitrogen/ethanol or nitrogen/isopropanol slush bath was used to maintain samples at the desired low temperature.

Variable-temperature (VT) NMR spectra were recorded on Bruker Avance 300, Bruker Avance 400 (Bruker, Billerica, MA, USA) and Varian Inova 400 (Varian, Palo Alto, CA, USA) spectrometers operating at 300 and 400 MHz in the 180–300 K temperature range. ^1H and $^{13}C\{^1H\}$, chemical shifts are reported in parts per million (ppm) downfield of tetramethylsilane (TMS) and were calibrated against the residual resonance of the deuterated solvent, while $^{31}P\{^1H\}$ chemical shifts were referenced to 85% H_3PO_4 with downfield shift taken as positive. The IR spectra were recorded at different temperatures (160–293 K) using a home-modified cryostat (Carl Zeiss Jena) with a Nicolet iS50 FTIR (Thermo Scientific, Waltham, MA, USA) spectrometer using 0.05 cm CaF_2 cells. The accuracy of the experimental temperature adjustment was ±0.5 °C. The cryostat modification allowed the transfer of the reagents (premixed at either low or room temperature) under an inert atmosphere directly into the cells.

Manganese hydride complexes *mer*,*trans*–$[(P(OPh)_3)_2Mn(CO)_3H]$ (**1**) [31], *mer*,*trans*–$[(PPh_3)_2Mn(CO)_3H]$ (**2**) [34], *fac*–$[(dppm)Mn(CO)_3H]$ (**3**) [27] and *fac*–$[(P\text{-}NHC)Mn(CO)_3H]$ (**4**) [4] (Scheme 2) were prepared according to the literature methods. Commercially

available tris(pentafluorophenyl)boron was purified by sublimation before use. All other reagent-grade chemicals purchased from commercial sources were used as received.

Synthesis of fac–[(P–NHC)Mn(CO)$_3$(MeCN)]BF$_4$ (4^{MeCN})

AgBF$_4$ (0.375 mmol, 73 mg) was placed into the Schlenk flask containing *fac*-(P-NHC)Mn(CO)$_3$Br (0.375 mmol, 226 mg) under inert atmosphere. Then 5 mL of CH$_3$CN was added upon stirring at room temperature. The obtained suspension was sonicated for 5 min and left stirring overnight till complete product formation that was controlled by the IR spectroscopy. After that, the CH$_3$CN was removed under reduced pressure, the yellow oil residue was dissolved in 5 mL of CH$_3$CN again to avoid colloid solution formation. The resulting solution was separated from the precipitate via filtration through a Pasteur pipette with Celite, concentrated to 1/10 of initial volume, and dry Et$_2$0 (80 mL) was added dropwise to induce precipitation of the product. The precipitate was left under supernatant overnight at −20 °C. The next day, the supernatant was removed, and the precipitate was washed with 5 mL two times and dried in a vacuum yielding (211 mg, 86%) pale-yellow powder.

Synthesis of mer,trans–[(PPh$_3$)$_2$Mn(CO)$_3$(CH$_3$CN)][BF$_4$] (2^{MeCN})

A suspension of (PPh$_3$)$_2$Mn(CO)$_3$H (0.008 mmol, 5.0 mg) and [Ph$_3$C][BF$_4$] (0.008 mmol, 2.6 mg) in CH$_3$CN (5 mL) was placed in the ultrasonic bath for 5 min at room temperature and left stirring till complete product formation that was controlled by the IR spectroscopy. The solvent was removed under reduced pressure. The resulting pale-yellow solid was dissolved in CH$_2$Cl$_2$ (1 mL) and then filtered through a Pasteur pipette with Celite. Hexane (5 mL) was added to the solution to induce crystallization. The supernatant was removed by decantation, the crystalline precipitate was washed with hexane (2 × 5 mL) and then dried in the vacuum to yield [(PPh$_3$)$_2$Mn(CO)$_3$(CH$_3$CN)][BF$_4$] (4.6 mg, 76%) as pale-yellow crystals.

Structures of reactants and complexes were optimized at the ωB97-XD level [35], applying def2-TZVP basis set [36] by Gaussian 09 [37]. Optimizations were done in toluene, THF and CH$_3$CN introduced by a SMD solvent model [38].

Cationic complexes *mer*,*trans*–[(PPh$_3$)$_2$Mn(CO)$_3$(MeCN)][BF$_4$] **2^{MeCN}** and *fac*–[(P–NHC)Mn(CO)$_3$(MeCN)][BF$_4$] **4^{MeCN}** were crystalized from the CH$_2$Cl$_2$/hexane system. X-ray diffraction data were collected at 100 K with a Bruker Quest D8 CMOS diffractometer (Bruker, MA, USA), using graphite monochromated Mo-Kα radiation (λ = 0.71073 Å). Using Olex2 [39], the structures were solved with the ShelXT [40] structure solution program using Intrinsic Phasing and refined with the XL [41] refinement package using Least-Squares minimization against F^2 in anisotropic approximation for non-hydrogen atoms. Positions of hydrogen atoms were calculated, and they were refined in the isotropic approximation within the riding model. Crystal data and structure refinement parameters are given in Table S2. CCDC 2241621 and 2241622 contain the supplementary crystallographic data for **2^{MeCN}** and **4^{MeCN}**, respectively.

3.1. General Procedure for the Interaction with Bases

For Variable Temperature IR Studies

The solution of *mer*,*trans*–[(P(OPh)$_3$)$_2$Mn(CO)$_3$H] (**1**, c = 0.003 M) was prepared at room temperature in methylcyclohexane. Then itthe was placed into a cryostat and cooled to 190 K. After the spectrum of the initial complex was acquired, the solution from the cryostat was added to the solution of corresponding base (pyridine, HMPA, DBU; 1–70 eq., c = 0.003–0.21 M dissolved in a small amount of solvent kept at 190 K in liquid nitrogen/*i*PrOH slush bath). The mixture obtained was quickly returned into the cryostat, and the IR spectra were monitored in the 190–290 K temperature range.

Solid *fac*–[(dppm)Mn(CO)$_3$H] (**3**, m = 10.0 mg, n = 0.02 mmol) and KHMDS (m = 11.5 mg, n = 0.10 mmol) were placed in separate Schlenk tubes under inert atmosphere. The complex was dissolved in THF or acetonitrile at room temperature, and a small aliquot was taken to IR cell. After the spectrum of the initial complex was acquired, the Schlenk tubes with

solution and solid KHMDS were cooled to 243 K in a liquid nitrogen/ethanol slush bath. Then the solution of complex **3** was quickly transferred to KHMDS with a Pasteur pipette, and the obtained mixture was stirred and transferred into the IR cell at room temperature for spectrum acquisition.

For Variable Temperature NMR Studies

Solid *fac*–[(dppm)Mn(CO)$_3$H] (**3**, m = 20 mg, n = 0.04 mmol) and KHMDS (m = 23 mg, n = 0.20 mmol) were placed in separate Schlenk tubes under inert atmosphere. The complex was dissolved in THF-d_8 or CD_3CN at room temperature. After that, the NMR tube under inert atmosphere and Schlenk tubes with solution and solid KHMDS were cooled to 243 K in a liquid nitrogen/ethanol slush bath. The solution of complex **3** was transferred to KHMDS with a Pasteur pipette, and the obtained mixture was stirred and quickly filtered through glass cotton directly into precooled NMR tube. The resulting NMR sample was inserted into a pre-cooled NMR probe at 243 K and then monitored with multi-nuclear NMR spectroscopy at 243 K.

3.2. General Procedure for the Interaction with Lewis Acid

For Variable Temperature NMR Studies

The chosen amount of *mer*,*trans*–[(P(OPh)$_3$)$_2$Mn(CO)$_3$H] (**1**, m = 5.3 mg, n = 0.007 mmol) was dissolved in toluene-d_8 at room temperature and monitored in the 200–293 K temperature range. Then the solution of B(C_6F_5)$_3$ (7 eq., m = 25 mg, n = 0.007 mmol in 0.5 mL toluene-d_8) was added at 200 K, and the reaction mixture was monitored at 200–293 K.

Similarly, complexes **2**–**4**, (m = 20 mg, n = 0.04 mmol) were dissolved in CD_2Cl_2, placed into an NMR tube and frozen in liquid nitrogen. Then the solution of the Lewis acid (B(C_6F_5)$_3$; 1 eq., n = 0.04 mmol) in CD_2Cl_2 was poured over the frozen solution in the NMR tube. Two frozen solutions were simultaneously melted in a slush nitrogen/EtOH bath at 180 K, and then the mixture obtained was monitored in the 183–293 K temperature range.

For Variable Temperature IR Studies

The solution of *mer*,*trans*–[(P(OPh)$_3$)$_2$Mn(CO)$_3$H] (**1**, c = 0.005 M) was prepared at room temperature in toluene. Then it was placed into a cryostat and cooled to 190 K. After the spectrum of the initial complex was acquired, the solution from the cryostat was added to B(C_6F_5)$_3$ (10 eq., c = 0.05 M) and dissolved in a small amount of solvent kept at 190 K in a nitrogen/*i*PrOH slush bath. The obtained mixture was quickly returned to the cryostat and monitored in the 190–290 K temperature range.

The solutions of complexes **2**–**4** (c = 0.003 M) were prepared at room temperature in *n*BuCl (CH_2Cl_2 or toluene). Then, they were placed into a cryostat and cooled to 160 K (180 K or 190 K). After the spectrum of the initial complex was acquired, the solution from the cryostat was added to the corresponding Lewis acid B(C_6F_5)$_3$ (1–1.3 eq., c = 0.003–0.004 M), dissolved in a small amount of solvent and cooled to 160 K (180 K or 190 K) in a nitrogen/EtOH (nitrogen/^{i}PrOH) slush bath. The obtained mixture was quickly returned to the cryostat and monitored in the 160 (180 or 190)–290 K temperature range.

4. Conclusions

In conclusion, we have shown that tricarbonyl manganese hydride complexes exhibit *dual* reactivity under *Lewis* acid or base treatment. Even the complexes with pronounced hydride character (**2**, **3**) can be deprotonated or, *vice versa*, the complex with acidic properties (**1**) can serve as a hydride donor. The Mn–H bond repolarization occurs at the stage of formation of non-covalent intermediates with *Lewis* acid or base as exemplified for complex **1**. The strength of these non-covalent bonds determines whether subsequent hydrogen ion (hydride or proton) transfer will occur. The studies on the complexes bearing bidentate ligands, *fac*–[(L–L′)Mn(CO)$_3$H] (**3**, **4**), revealed that their reactions do not follow simple mechanisms but rather involve the *fac*-to-*mer* isomerizations. The hydride abstraction from these hydrides proceeds from the *mer*-derivatives in which the hydride ligand located *trans* to electron-donating phosphine ligand is more reactive relative to *fac*-isomers where

hydride is *trans* to CO ligand. Interestingly, the initial deprotonation site of complex **3** in acetonitrile was observed at the CH_2 bridge of the dppm ligand, providing the expected metal-deprotonated product via proton migration from anionic hydride intermediate. Since anionic or cationic Mn(I) complexes formed as the result of proton or hydride abstraction are potential intermediates of (de)hydrogenation reactions, quantitative values of kinetic hydricity of the hydride complexes obtained herein may correlate with their potential catalytic activity and be useful for further elucidation of reaction mechanisms.

Supplementary Materials: The following supporting information can be downloaded at: https://www.mdpi.com/article/10.3390/molecules28083368/s1: IR and NMR spectroscopic characterization of Mn(I) hydride, cationic and anionic complexes; crystal data and structure refinement parameters; details of thermodynamic and kinetic parameters determination.

Author Contributions: Investigation, E.S.O., S.A.K., E.S.G., N.V.K., A.A.P., O.A.F., D.A.V. and A.A.D.; Writing—Original Draft Preparation, E.S.O.; Writing—Review and Editing, N.V.B., D.A.V. and Y.C.; Supervision, E.S.S. and N.V.B. All authors have read and agreed to the published version of the manuscript.

Funding: This work was financially supported by the Russian Science Foundation (grant No. 22-73-00072).

Institutional Review Board Statement: Not applicable.

Informed Consent Statement: Not applicable.

Data Availability Statement: The data presented in this study are available in the article or Supplementary Materials.

Acknowledgments: D.A.V. and Y.C. thank CNRS for the support. E.S.G. is grateful to the French Embassy in Moscow for a joint PhD fellowship (Vernadski program). Computational studies were performed using HPC resources from CALMIP (grant no. P18038). The NMR and X-ray diffraction data were collected using the equipment of the Center for Molecular Composition Studies of INEOS RAS with the support from the Ministry of Science and Higher Education of the Russian Federation (Contract No. 075-03-2023-642).

Conflicts of Interest: The authors declare no conflict of interest.

Sample Availability: Samples of the compounds are not available from the authors.

References

1. Valyaev, D.A.; Lavigne, G.; Lugan, N. Manganese organometallic compounds in homogeneous catalysis: Past, present, and prospects. *Coord. Chem. Rev.* **2016**, *308*, 191–235. [CrossRef]
2. Mukherjee, A.; Milstein, D. Homogeneous catalysis by cobalt and manganese pincer complexes. *ACS Catal.* **2018**, *8*, 11435–11469. [CrossRef]
3. Gulyaeva, E.S.; Osipova, E.S.; Buhaibeh, R.; Canac, Y.; Sortais, J.-B.; Valyaev, D.A. Towards ligand simplification in manganese-catalyzed hydrogenation and hydrosilylation processes. *Coord. Chem. Rev.* **2022**, *458*, 214421. [CrossRef]
4. Buhaibeh, R.; Filippov, O.A.; Bruneau-Voisine, A.; Willot, J.; Duhayon, C.; Valyaev, D.A.; Lugan, N.; Canac, Y.; Sortais, J.B. Phosphine-NHC manganese hydrogenation catalyst exhibiting a non-classical metal-ligand cooperative H_2 activation mode. *Angew. Chem. Int. Ed.* **2019**, *131*, 6799–6803. [CrossRef]
5. Kireev, N.V.; Filippov, O.A.; Gulyaeva, E.S.; Shubina, E.S.; Vendier, L.; Canac, Y.; Sortais, J.-B.; Lugan, N.; Valyaev, D.A. Bis[diphenylphosphino]methane and its bridge-substituted analogues as chemically non-innocent ligands for H_2 activation. *Chem. Commun.* **2020**, *56*, 2139–2142. [CrossRef]
6. Pearson, R.G. The transition-metal-hydrogen bond. *Chem. Rev.* **1985**, *85*, 41–49. [CrossRef]
7. Crabtree, R.H. *The Organometallic Chemistry of the Transition Metals*; John Wiley & Sons: Hoboken, NJ, USA, 2009.
8. Kristjánsdóttir, S.; Norton, J. *Transition Metal Hydrides*; Dedieu, A., Ed.; VCH: New York, NY, USA, 1992; Volume 309.
9. Bullock, R.M. Catalytic ionic hydrogenations. *Chem. Eur. J.* **2004**, *10*, 2366–2374. [CrossRef]
10. Jordan, R.F.; Norton, J.R. Kinetic and thermodynamic acidity of hydrido transition-metal complexes. 1. Periodic trends in Group VI complexes and substituent effects in osmium complexes. *J. Am. Chem. Soc.* **1982**, *104*, 1255–1263. [CrossRef]
11. Cheng, T.-Y.; Brunschwig, B.S.; Bullock, R.M. Hydride transfer reactions of transition metal hydrides: Kinetic hydricity of metal carbonyl hydrides. *J. Am. Chem. Soc.* **1998**, *120*, 13121–13137. [CrossRef]
12. Bullock, R.M. Proton transfer from metal hydrides to metal alkynyl complexes. Remarkable carbon basicity of $(C_5H_5)(PMe_3)_2Ru$-CC-CMe_3. *J. Am. Chem. Soc.* **1987**, *109*, 8087–8089. [CrossRef]

13. Filippov, O.; Golub, I.; Osipova, E.; Kirkina, V.; Gutsul, E.; Belkova, N. Activation of M—H bond upon the complexation of transition metal hydrides with acids and bases. *Russ. Chem. Bull.* **2014**, *63*, 2428–2433. [CrossRef]
14. Belkova, N.V.; Filippov, O.A.; Osipova, E.S.; Safronov, S.V.; Epstein, L.M.; Shubina, E.S. Influence of phosphine (pincer) ligands on the transition metal hydrides reactivity. *Coord. Chem. Rev.* **2021**, *438*, 213799. [CrossRef]
15. Wiedner, E.S.; Chambers, M.B.; Pitman, C.L.; Bullock, R.M.; Miller, A.J.; Appel, A.M. Thermodynamic hydricity of transition metal hydrides. *Chem. Rev.* **2016**, *116*, 8655–8692. [CrossRef]
16. Edidin, R.T.; Sullivan, J.M.; Norton, J.R. Kinetic and thermodynamic acidity of hydrido transition-metal complexes. 4. Kinetic acidities toward aniline and their use in identifying proton-transfer mechanisms. *J. Am. Chem. Soc.* **1987**, *109*, 3945–3953. [CrossRef]
17. Sandhya, K.; Suresh, C.H. Quantification of thermodynamic hydridicity of hydride complexes of Mn, Re, Mo, and W using the molecular electrostatic potential. *J. Phys. Chem.* **2017**, *121*, 2814–2819. [CrossRef]
18. Kuchynka, D.; Amatore, C.; Kochi, J. Electrooxidation of metal cabonyl anions. Formation and reactivity of 17-electron manganese (0) radicals. *J. Organomet. Chem.* **1987**, *328*, 133–154. [CrossRef]
19. Belkova, N.V.; Epstein, L.M.; Filippov, O.A.; Shubina, E.S. Hydrogen and dihydrogen bonds in the reactions of metal hydrides. *Chem. Rev.* **2016**, *116*, 8545–8587. [CrossRef]
20. Belkova, N.V.; Epstein, L.M.; Shubina, E.S. Dihydrogen bonding, proton transfer and beyond: What we can learn from kinetics and thermodynamics. *Eur. J. Inorg. Chem.* **2010**, *23*, 3555–3565. [CrossRef]
21. Ault, B.S.; Becker, T.M.; Li, G.Q.; Orchin, M. The infrared spectra and theoretical calculations of frequencies of fac-tricarbonyl octahedral complexes of manganese (I). *Spectrochim. Acta A Mol. Biomol. Spectrosc.* **2004**, *60*, 2567–2572. [CrossRef]
22. Belkova, N.V.; Gutsul, E.I.; Filippov, O.A.; Levina, V.A.; Valyaev, D.A.; Epstein, L.M.; Lledos, A.; Shubina, E.S. Intermolecular hydrogen bonding between neutral transition metal hydrides (η^5-C_5H_5)M(CO)$_3$H (M = Mo, W) and bases. *J. Am. Chem. Soc.* **2006**, *128*, 3486–3487. [CrossRef] [PubMed]
23. Levina, V.A.; Filippov, O.A.; Gutsul, E.I.; Belkova, N.V.; Epstein, L.M.; Lledos, A.; Shubina, E.S. Neutral transition metal hydrides as acids in hydrogen bonding and proton transfer: Media polarity and specific solvation effects. *J. Am. Chem. Soc.* **2010**, *132*, 11234–11246. [CrossRef]
24. Levina, V.A.; Rossin, A.; Belkova, N.V.; Chierotti, M.R.; Epstein, L.M.; Filippov, O.A.; Gobetto, R.; Gonsalvi, L.; Lledós, A.; Shubina, E.S. Acid–base interaction between transition-metal hydrides: Dihydrogen bonding and dihydrogen evolution. *Angew. Chem. Int. Ed.* **2011**, *123*, 1403–1406. [CrossRef]
25. Osipova, E.S.; Belkova, N.V.; Epstein, L.M.; Filippov, O.A.; Kirkina, V.A.; Titova, E.M.; Rossin, A.; Peruzzini, M.; Shubina, E.S. Dihydrogen bonding and proton transfer from MH and OH acids to Group 10 metal hydrides [(^{tBu}PCP)MH][^{tBu}PCP = κ^3-2,6-(*t*Bu$_2$PCH$_2$)$_2$C$_6$H$_3$; M = Ni, Pd]. *Eur. J. Inorg. Chem.* **2016**, *2016*, 1415–1424. [CrossRef]
26. Eckert, F.; Leito, I.; Kaljurand, I.; Kütt, A.; Klamt, A.; Diedenhofen, M. Prediction of acidity in acetonitrile solution with COSMO-RS. *J. Comput. Chem.* **2009**, *30*, 799–810. [CrossRef] [PubMed]
27. Osipova, E.S.; Gulyaeva, E.S.; Kireev, N.V.; Kovalenko, S.A.; Bijani, C.; Canac, Y.; Valyaev, D.A.; Filippov, O.A.; Belkova, N.V.; Shubina, E.S. Fac-to-mer isomerization triggers hydride transfer from Mn (I) complex fac-[(dppm)Mn(CO)$_3$H]. *Chem. Comm.* **2022**, *58*, 5017–5020. [CrossRef]
28. Kaljurand, I.; Kütt, A.; Sooväli, L.; Rodima, T.; Mäemets, V.; Leito, I.; Koppel, I.A. Extension of the self-consistent spectrophotometric basicity scale in acetonitrile to a full span of 28 pKa units: Unification of different basicity scales. *J. Org. Chem.* **2005**, *70*, 1019–1028. [CrossRef]
29. Tabassum, S.; Sereda, O.; Reddy, P.V.G.; Wilhelm, R. Hindered Brønsted bases as Lewis base catalysts. *Org. Biomol. Chem.* **2009**, *7*, 4009–4016. [CrossRef]
30. Narayanan, B.; Amatore, C.; Kochi, J. Electroreduction of carbonylmanganese (I) cations. Mechanism of ligand substitution and hydride formation via manganese (0) intermediates. *Organometallics.* **1987**, *6*, 129–136. [CrossRef]
31. Booth, B.; Haszeldine, R. Metal carbonyl chemistry. Part I. The reactions of phosphorus-containing ligands with hydridopentacarbonylmanganese. *J. Chem. Soc. A* **1966**, 157–160. [CrossRef]
32. Danopoulos, A.A.; Pugh, D.; Smith, H.; Saßmannshausen, J. Structural and reactivity studies of "pincer" pyridine dicarbene complexes of Fe0: Experimental and computational comparison of the phosphine and NHC donors. *Chem. Eur. J.* **2009**, *15*, 5491–5502. [CrossRef]
33. Zhen, Y.; Feighery, W.G.; Lai, C.K.; Atwood, J.D. Steric and electronic factors that control two-electron processes between metal carbonyl cations and anions. *J. Am. Chem. Soc.* **1989**, *111*, 7832–7837. [CrossRef]
34. Mandal, S.K.; Feldman, J.; Orchin, M. A New route to manganese and rhenium carbonyl tetrafluoroborate salts and an improved procedure for preparing their precursor hydrides. *J. Coord. Chem.* **1994**, *33*, 219–221. [CrossRef]
35. Chai, J.-D.; Head-Gordon, M. Long-range corrected hybrid density functionals with damped atom–atom dispersion corrections. *Phys. Chem. Chem. Phys.* **2008**, *10*, 6615–6620. [CrossRef] [PubMed]
36. Weigend, F.; Ahlrichs, R. Balanced basis sets of split valence, triple zeta valence and quadruple zeta valence quality for H to Rn: Design and assessment of accuracy. *Phys. Chem. Chem. Phys.* **2005**, *7*, 3297–3305. [CrossRef]
37. Frisch, M.J.; Trucks, G.W.; Schlegel, H.B.; Scuseria, G.E.; Robb, M.A.; Cheeseman, J.R.; Montgomery, J.J.A.; Vreven, T.; Kudin, K.N. *Gaussian 09, Revision D.1*; Gaussian, Inc.: Wallingford, CT, USA, 2009.

38. Marenich, A.V.; Cramer, C.J.; Truhlar, D.G. Universal solvation model based on solute electron density and on a continuum model of the solvent defined by the bulk dielectric constant and atomic surface tensions. *J. Phys. Chem. B* **2009**, *113*, 6378–6396. [CrossRef]
39. Dolomanov, O.V.; Bourhis, L.J.; Gildea, R.J.; Howard, J.A.; Puschmann, H. OLEX2: A complete structure solution, refinement and analysis program. *J. Appl. Crystallogr.* **2009**, *42*, 339–341. [CrossRef]
40. Sheldrick, G.M. SHELXT–Integrated space-group and crystal-structure determination. *Acta Crystallogr. A* **2015**, *71*, 3–8. [CrossRef]
41. Sheldrick, G.M. A short history of SHELX. *Acta Crystallogr. A* **2008**, *64*, 112–122. [CrossRef]